

A Novel Self-generating Liquid MOCVD Precursor for Co_3O_4 Thin Films

Antonino Gulino,^{*,†} Paolo Dapporto,[‡]
Patrizia Rossi,[‡] and Ignazio Fragalà^{*,†}

*Dipartimento di Scienze Chimiche, Università di Catania and I.N.S.T.M. UdR of Catania,
V.le A. Doria 6, 95125 Catania, Italy, and
Dipartimento di Energetica, Università di Firenze,
V. Santa Marta 3, 50139 Firenze, Italy*

Received April 29, 2003
Revised Manuscript Received July 8, 2003

Materials based on cobalt oxides have been extensively investigated because of their potential application in many technological fields.¹

The cobalt oxide system includes CoO , Co_3O_4 , Co_2O_3 , and CoO_2 .^{1–4} The mixed $\text{Co}(\text{II})$ – $\text{Co}(\text{III})$ Co_3O_4 constitutes the most studied compound in view of application as optical gas sensors,⁵ catalysts in oxidation reactions,⁶ electrochromic devices,^{7,8} high-temperature solar selective absorbers,⁹ and magnetic materials.¹⁰

Co_3O_4 shows the spinel structure based on a cubic close packing array of oxide ions where one-eighth of tetrahedral holes are occupied by $\text{Co}(\text{II})$ ions and one-half of octahedral holes are occupied by $\text{Co}(\text{III})$ ions.^{11,12}

* Corresponding author. Fax: ++39-095-580138. E-mail: agulino@
dipchi.unict.it (A. Gulino).

[†] Università di Catania.

[‡] Università di Firenze.

(1) (a) *Oxide Surfaces – The Chemical Physics of Solid Surfaces*, Woodruff, D. P., Ed.; Elsevier: Amsterdam, 2001; Vol. 9. (b) Choy, J. H.; Jung, H.; Han, Y.-S.; Yoon, J.-B.; Shul, Y.-G.; Kim, H.-J. *Chem. Mater.* **2002**, *14*, 3823. (c) Venkatakrishnan, S.; Manthiram, A. *Chem. Mater.* **2002**, *14*, 3907. (d) Levasseur, S.; Menetrier, M.; Delmas, C. *Chem. Mater.* **2002**, *14*, 3584. (e) Pan, C.; Lee, Y. J.; Ammundsen, B.; Grey, C. P. *Chem. Mater.* **2002**, *14*, 2289. (b) Cho, J.; Kim, Y. J.; Kim, T. J.; Park, B. *Angew. Chem. Int. Ed.* **2001**, *40*, 3367 and references therein. (g) Sampanthar, J. T.; Zeng, H. C. *Chem. Mater.* **2001**, *13*, 4722. (h) Ji, L.; Lin, J.; Zeng, H. C. *Chem. Mater.* **2000**, *12*, 3466. (i) Xu, Z. P.; Zeng, H. C. *Chem. Mater.* **2000**, *12*, 3459. (j) Kumar, R. V.; Diamant, Y.; Gedanken, A. *Chem. Mater.* **2000**, *12*, 2301. (k) Yan, H.; Blanford, C. F.; Holland, B. T.; Smyrl, W. H.; Stein, A. *Chem. Mater.* **2000**, *12*, 1134. (l) Chellam, U.; Xu, Z. P.; Zeng, H. C. *Chem. Mater.* **2000**, *12*, 650. (m) Rojas, R. M.; Kovacheva, D.; Petrov, K. *Chem. Mater.* **1999**, *11*, 3263. (n) Trinschek, D.; Jansen, M. *Angew. Chem., Int. Ed.* **1999**, *38*, 133 and references therein. (o) Reetz, M. T.; Quaizer, S. A.; Winter, M.; Becker, J. A.; Joerg, A.; Schaefer, R.; Stimming, U.; Marmann, A.; Vogel, R.; Konno, T. *Angew. Chem., Int. Ed. Engl.* **1996**, *35*, 2092 and references therein.

(2) Shen, Z.-X.; Allen, J. W.; Lindberg, P. A. P.; Dessau, D. S.; Wells, B. O.; Borg, A.; Ellis, W.; Kang, J. S.; Oh, S.-J.; Lindau, I.; Spicer, W. E. *Phys. Rev. B* **1990**, *42*, 1817.

(3) Choi, J. S.; Yo, C. H. *Inorg. Chem.* **1974**, *13*, 1720.

(4) Patil, P. S.; Kadam, L. D.; Lokhande C. D. *Thin Solid Films* **1996**, *272*, 29.

(5) (a) Ando, M.; Kobayashi, T.; Iijima, S.; Haruta, M. *J. Mater. Chem.* **1997**, *7*, 1779. (b) Yamaura, H.; Tamaki, J.; Moriya, K.; Miura, N.; Yamazoe, N. *J. Electrochem. Soc.* **1997**, *144*, L158.

(6) (a) Natile, M. M.; Glisenti, A. *Chem. Mater.* **2002**, *14*, 3090. (b) Hoffmann, C.; Wolf, A.; Schuth, F. *Angew. Chem., Int. Ed.* **1999**, *38*, 2800 and references therein. (c) Christoskova, St. G.; Stoyanova, M.; Georgieva, M.; Mehandjiev, D. *Mater. Chem. Phys.* **1999**, *60*, 39. (d) Nkeng, P.; Koenig, J.; Gautier, J.; Chartier, P.; Poillerat, G. *J. Electroanal. Chem.* **1996**, *402*, 81.

(7) (a) Seike, T.; Nagai, J. *Sol. Energy Mater.* **1991**, *22*, 107. (b) Švegl, F.; Orel, B.; Hutchins, M. G.; Kalcher, K. *J. Electrochem. Soc.* **1996**, *143*, 1532. (c) Maruyama, T.; Arai, S. *J. Electrochem. Soc.* **1996**, *143*, 1383.

(8) Granqvist, C. G. *Handbook of Inorganic Electrochromic Materials*; Elsevier: Amsterdam, 1995.

Many studies have been reported for preparation of bulk,^{1,6,a,c,9,10,13} thin films,^{4,5,a,b,7,8,a–b,d–g,14,15} and nanotubes¹⁶ of Co oxides as sol–gel, spray pyrolysis, electron beam evaporation, electrodeposition, oxidation of Co, pulsed laser deposition, radio frequency reactive sputtering, and so forth, including some examples of metal organic chemical vapor deposition^{7c,15} (MOCVD).

In this context, there is enough motivation to further investigate the synthesis of novel liquid precursors better suited for MOCVD of Co_3O_4 thin films. Therefore, in the present communication we report on the novel $\text{Co}(\text{C}_5\text{F}_6\text{HO}_2)_2 \cdot 2\text{H}_2\text{O} \cdot \text{CH}_3(\text{OCH}_2\text{CH}_2)_4\text{OCH}_3$ liquid adduct which, in addition, has proven to be a well-suited precursor for MOCVD of Co_3O_4 films. Obviously, MOCVD from liquid precursors certainly represents an issue of considerable relevance because of the accurate reproducibility associated with constant evaporation (hence constant mass transport) rates for given source temperatures.

The $\text{Co}(\text{C}_5\text{F}_6\text{HO}_2)_2 \cdot 2\text{H}_2\text{O} \cdot \text{CH}_3(\text{OCH}_2\text{CH}_2)_4\text{OCH}_3$ adduct (m.w. 731.34) (hereafter $\text{Co}(\text{hfac})_2 \cdot 2\text{H}_2\text{O} \cdot \text{tetraglyme}$

(9) (a) Barrera, E.; Gonzalez, I.; Viveros, T. *Sol. Energy Mater. Sol. Cells* **1998**, *51*, 69. (b) Hutchins, M. G.; Wright, P. J.; Grebenik, P. D. *Sol. Energy Mater.* **1987**, *16*, 113. (c) Cook, J. G.; Koffyberg, F. P. *Sol. Energy Mater.* **1984**, *10*, 55. (d) McDonald, G. E. *Thin Solid Films* **1980**, *72*, 83. (e) Smith, G. B.; Ignatiev, A.; Zajac, G. *J. Appl. Phys.* **1980**, *51*, 4186. (f) Cathro, K. J. *Sol. Energy Mater.* **1984**, *9*, 433. (g) Chidambaram, K.; Malhotra, K. L.; Chopra, K. L. *Thin Solid Films* **1982**, *87*, 365.

(10) (a) Verelst, M.; Ely, T. O.; Amiens, C.; Snoeck, E.; Lecante, P.; Mosset, A.; Respaud, M.; Broto, J. M.; Chaudret, B. *Chem. Mater.* **1999**, *11*, 2702.

(11) Mocuta, C.; Barbier, A.; Renaud, G. *Appl. Surf. Sci.* **2000**, *162*–163, 56.

(12) Wells, A. F. *Structural Inorganic Chemistry 4*; Clarendon Press: Oxford, 1975.

(13) (a) Zeng, H. C.; Lim, Y. Y. *J. Mater. Res.* **2000**, *15*, 1250. (b) Lakshmi, B. B.; Patrissi, C. J.; Martin, C. R. *Chem. Mater.* **1997**, *9*, 2544. (c) Gazzoli, D.; Occhiuzzi, M.; Cimino, A.; Cordischi, D.; Minelli, G.; Pinzari, F. *J. Chem. Soc., Faraday Trans.* **1996**, *92*, 4567. (d) El Baydi, M.; Poillerat, G.; Rehspringer, J.; Gautier, J. L.; Koenig, J.; Chartier, P. *J. Solid State Chem.* **1994**, *109*, 281.

(14) (a) Pejova, B.; Isahi, A.; Najdoski, M.; Grozdanov, I. *Mater. Res. Bull.* **2001**, *36*, 161. (b) Barrera, E.; Viveros, T.; Avila, A.; Quintana, P.; Morales, M.; Batina, N. *Thin Solid Films* **1999**, *346*, 138. (c) Ando, M.; Kobayashi, T. *Solid State Ionics* **2000**, *136*–137, 1291. (d) Gazzadi, G. C.; Borghi, A.; Di Bona, A.; Valeri, S. *Surf. Sci.* **1998**, *402*–404, 632. (e) Heiler, M.; Chassé, A.; Schindler, K.-M.; Hollering, M.; Neddermeyer, H. *Surf. Sci.* **2000**, *454*–456, 36. (f) Tanaka, M.; Mukai, M.; Fujimori, Y.; Kondoh, M.; Tasaka, Y.; Baba, H.; Usami, S. *Thin Solid Films* **1996**, *281*–282, 453. (g) Borghi, A.; Di Bona, A.; Bisero, D.; Valeri, S. *Appl. Surf. Sci.* **1999**, *150*, 13. (h) Armelao, L.; Barreca, D.; Grossi, S.; Martucci, A.; Tieto, M.; Tondello, E. *J. Non-Cryst. Solid.* **2001**, *293*–295, 477. (i) Valeri, S.; Borghi, A.; Gazzadi, G. C.; Di Bona, A. *Surf. Sci.* **1999**, *423*, 346. (j) Sebastian, I.; Neddermeyer, H. *Surf. Sci.* **2000**, *454*–456, 771. (k) Singh, R. N.; Hamdani, M.; Koenig, J.; Poillerat, G.; Gautier, J. *J. Appl. Electrochem.* **1990**, *20*, 442. (l) Koyano, G.; Watanabe, H.; Okuhara, T.; Misono, M. *J. Chem. Soc., Faraday Trans.* **1996**, *92*, 3425.

(15) (a) Barreca, D.; Massignan, C.; Daolio, S.; Fabrizio, M.; Piccirillo, C.; Armelao, L.; Tondello, E. *Chem. Mater.* **2001**, *13*, 588. (b) Shalini, K.; Anil, U. M.; Shivashankar, S. A.; Rajeswari, M.; Choopun, S. *J. Cryst. Growth* **2001**, *231*, 242. (c) Holgado, J. P.; Caballero, A.; Espinos, J. P.; Morales, J.; Jimenez, V. M.; Justo, A.; Gonzalez-Elipe, A. R. *Thin Solid Films* **2000**, *377*, 460. (d) Cheng, C.-S.; Serizawa, M.; Sakata, H.; Hirayama, T. *Mater. Chem. Phys.* **1998**, *53*, 225. (e) Maruyama, T.; Nakai, T. *Sol. Energy Mater.* **1991**, *23*, 25. (f) Colombo, D. G.; Gilmer, D. C.; Young, V. G.; Campbell, S. A.; Gladfelter, W. L. *Chem. Vap. Deposition* **1998**, *4*, 220. (g) Fujii, E.; Tomazawa, A.; Fujii, S.; Torii, H.; Hattori, M.; Takayama, R. *Jpn. J. Appl. Phys.* **1993**, *32*, L1448. (h) Fujii, E.; Torii, H.; Tomazawa, A.; Takayama, R.; Hirao, T. *J. Mater. Sci.* **1995**, *30*, 6013.

(16) Shi, X.; Han, S.; Sanedrin, R. J.; Zhou, F.; Selke M. *Chem. Mater.* **2002**, *14*, 1897.

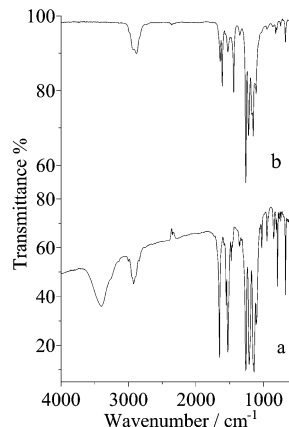


Figure 1. FT-IR spectrum of $\text{Co}(\text{hfac})_2 \cdot 2\text{H}_2\text{O} \cdot \text{tetraglyme}$: (a) in KBr; (b) gas phase.

(tetraglyme = 2,5,8,11,14-pentaoxapentadecane and $\text{C}_5\text{F}_6\text{HO}_2$ = hexafluoroacetylacetone = 1,1,1,5,5,5-hexafluoro-2-4-pentanedionate = hfac) was synthesized by adding, under vigorous stirring, 0.465 g (0.005 mol) of $\text{Co}(\text{OH})_2$, 1.42 mL (0.01 mol) of H-hfac, and 1.1 mL of tetraglyme (0.005 mol) to 45 mL of CH_2Cl_2 . The suspension was stirred and refluxed at 40 °C for 4 h. An excess of $\text{Co}(\text{OH})_2$ was filtered off. A brown oil was obtained after evaporation of the CH_2Cl_2 solvent. Yield: 72%. Brown, transparent crystals resulted by dissolving the oil in 50 mL of hexane and leaving the solution to concentrate to room temperature. A similar synthetic procedure carried out with CoO instead of $\text{Co}(\text{OH})_2$ gave much lower yield. This behavior has been previously reported also for the synthesis of $\text{Zn}(\text{hfac})_2$ adducts.¹⁷ $\text{Co}(\text{OH})_2$ was, therefore, freshly prepared by dropwise addition of a dilute NaOH solution to $\text{Co}(\text{NO}_3)_2 \cdot 6\text{H}_2\text{O}$ dissolved in H_2O . The hydroxide gel thus formed was filtered off, washed with distilled water, and dried overnight at room temperature. Melting point of the $\text{Co}(\text{hfac})_2 \cdot 2\text{H}_2\text{O} \cdot \text{tetraglyme}$ product: 57 °C. Elemental analysis for $\text{CoC}_{20}\text{H}_{28}\text{F}_{12}\text{O}_{11}$. Calcd: C, 32.84; H, 3.86. Found: C, 33.02; H, 3.89%. Electron impact mass spectrum (EI-MS, 70 eV, m/z fragments; M = $\text{Co}(\text{hfac})_2 \cdot \text{tetraglyme}$): 488 (10%) ($\text{M} - \text{hfac}$)⁺, 473 (75%) ($\text{M} - \text{tetraglyme}$)⁺, 404 (100%) ($\text{M} - \text{tetraglyme} - \text{CF}_3$)⁺, 266 (55%) ($\text{M} - \text{tetraglyme} - \text{hfac}$)⁺, 216 (50%) ($\text{M} - \text{tetraglyme} - \text{hfac} - \text{CF}_2$)⁺. The main observed groups are due to the loss of tetraglyme and hfac fragments. The $\text{Co}(\text{hfac})_2$ ion peak is at $m/z = 473$. These observed fragments, as well as the evidence of fluorine group transfer processes, have already been reported in mass spectra of closely related systems.^{17–20} Infrared transmittance spectrum (Figure 1a) IR (KBr; ν/cm^{-1}): 3400 (m), 3270 (sh), 3140 (sh), 3005 (w), 2948 (sh), 2927 (m), 2890 (sh), 2842 (w), 1738 (w), 1645 (s), 1620 (sh), 1583 (w), 1554 (s), 1530 (s), 1472 (m), 1357 (w), 1325 (vw), 1259 (s), 1210 (s), 1157 (s), 1136 (sh), 1108 (s), 1050 (vw), 1026 (m), 948 (m), 924 (sh), 850 (m), 813 (w), 792 (m),

(17) (a) Gulino, A.; Fiorito, G.; Fragalà, I. *J Mater. Chem.* **2003**, 13, 861. (b) Gulino, A.; Castelli, F.; Dapporto, P.; Rossi, P.; Fragalà, I. *Chem. Mater.* **2000**, 12, 548

(18) Gulino, A.; Castelli, F.; Dapporto, P.; Rossi, P.; Fragalà, I. *Chem. Mater.* **2002**, 14, 704.

(19) Gulino, A.; Dapporto, P.; Rossi, P.; Fragalà, I. *Chem. Mater.* **2002**, 14, 1442.

(20) Gulino, A.; Dapporto, P.; Rossi, P.; Fragalà, I. *Chem. Mater.* **2002**, 14, 4955.

768 (vw), 743 (vw), 669 (m).²¹ The nature of vapors evaporating from the $\text{Co}(\text{hfac})_2 \cdot 2\text{H}_2\text{O} \cdot \text{tetraglyme}$ melt system has been investigated by low-pressure (10 Torr) gas-phase FT-IR experiments. No sizable IR signals are detected up to 60 °C. Signals grow in the 65–180 °C temperature range and the resulting IR spectrum is diagnostic of the anhydrous $\text{Co}(\text{hfac})_2 \cdot \text{tetraglyme}$ system (Figure 1b). In fact, (i) there is no evidence of the H_2O stretching modes;¹⁷ (ii) the bands in the 2982–2815 cm^{-1} range are associated with the C–H (tetraglyme) stretching modes;²⁰ and even more important, (iii) the relative ratios of absorbances associated to C–H tetraglyme modes (2982–2815 cm^{-1}) and to the hfac C=O stretching (1645 cm^{-1}) remain strictly constant in the entire 65–180 °C temperature range. This observation, in addition, appears consistent with competing H_2O and tetraglyme ancillary ligation upon melting, beyond 57 °C, the latter being favored in the melt.

The configuration of the $[\text{Co}(\text{hfac})_2 \cdot 2\text{H}_2\text{O} \cdot \text{tetraglyme}]$ was determined through single-crystal X-ray structure analysis. Crystallographic data for $\text{Co}(\text{hfac})_2 \cdot 2\text{H}_2\text{O} \cdot \text{tetraglyme}$ were collected on a Siemens SMART diffractometer equipped with a rotating anode and controlled using the SMART software.²² The radiation used was Cu K α ($\lambda = 1.5418 \text{ \AA}$) and the intensities were collected at 150 K. Five settings of ϖ were used and narrow data "frames" were collected for 0.3° increments in ϖ . A total of 3000 frames of data were collected, providing a sphere of data. Data reduction was performed with the SAINT 4.0 program.²³

$\text{Co}(\text{hfac})_2 \cdot 2\text{H}_2\text{O} \cdot \text{tetraglyme}$ crystallizes in the monoclinic crystal system, space group $P21/n$, $Z = 4$, cell dimensions $a = 17.5346(6) \text{ \AA}$, $b = 7.9586(4) \text{ \AA}$, $c = 22.6169(8) \text{ \AA}$, $\beta = 110.040(2)^\circ$, $V = 2965.1(2) \text{ \AA}^3$, $\rho_{\text{calcd}} = 1.634 \text{ g/cm}^3$, $F(000) = 1484$. The structure was refined to a final R -factor of 0.0704 based on 2878 independent reflections having $I > 2\sigma(I)$ (417 refined parameters).

The structure was solved by direct methods using the SIR97 program²⁴ and refined by full-matrix least-squares against F^2 using all data (SHELX97).²⁵ An absorption correction to all data was applied, SADABS.²⁶ Atomic scattering factors and anomalous dispersion corrections for all the atoms were taken from ref 27.

Anisotropic thermal parameters were used for the non H-atoms. All the hydrogen atoms of hfac anions and of the polyether molecule were introduced in calculated positions with their temperature factors refined accordingly to the corresponding values of their bonded atoms; the overall temperature factor converged to 0.050(4) \AA^2 . The hydrogen atoms of water molecules were found in the Fourier difference map and their positions were

(21) Morris, M. L.; Moshier, R. W.; Sievers, R. E. *Inorg. Chem.* **1963**, 2, 411.

(22) SMART: Area-Detector Integration Software; Siemens Industrial Automation, Inc.: Madison, WI, 1995.

(23) SAINT Version 4.0; Siemens Industrial Automation, Inc.: Madison, WI, 1995.

(24) Altomare, A.; Cascarano, G. L.; Giacovazzo, C.; Guagliardi, A.; Burla, M. C.; Polidori, G.; Camalli, M. *J. Appl. Crystallogr.* **1999**, 32, 115.

(25) Sheldrick, G. M. SHELX 97; University of Göttingen: Göttingen, Germany, 1997.

(26) Sheldrick, G. M. SADABS; University of Göttingen: Göttingen, Germany, 1996.

(27) International Tables for X-ray Crystallography; Kynoch Press: Birmingham, UK, 1974; Vol. 4.

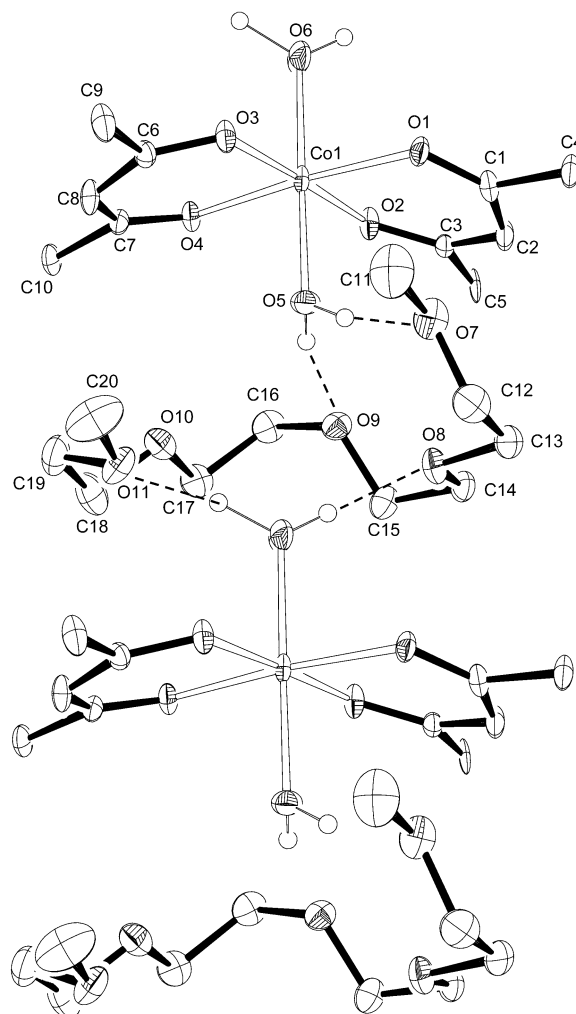


Figure 2. ORTEP drawing of the $\text{Co}(\text{hfac})_2 \cdot 2\text{H}_2\text{O} \cdot \text{tetraglyme}$.

Table 1. Selected Bond Distances (Å) and Angles (deg) for $\text{Co}(\text{hfac})_2 \cdot 2\text{H}_2\text{O} \cdot \text{tetraglyme}$

Co1–O1	2.075(4)	O1–Co1–O2	88.4(1)
Co1–O2	2.070(4)	O1–Co1–O3	93.9(2)
Co1–O3	2.065(4)	O1–Co1–O4	175.4(2)
Co1–O4	2.066(4)	O1–Co1–O5	87.5(2)
Co1–O5	2.096(5)	O1–Co1–O6	90.5(2)
Co1–O6	2.072(5)	O2–Co1–O3	177.5(2)
		O2–Co1–O4	88.9(2)
		O2–Co1–O5	92.0(2)
		O2–Co1–O6	90.2(2)
		O3–Co1–O4	88.8(2)
		O3–Co1–O5	87.1(2)
		O3–Co1–O6	90.8(2)
		O4–Co1–O5	88.9(2)
		O4–Co1–O6	93.2(2)
		O5–Co1–O6	177.1(2)

refined as well as their isotropic displacement parameters.

Geometrical calculations were performed by PARST97²⁸ and a molecular plot was produced by the program ORTEP3.²⁹ Crystal and structure refinement data are collected in Table S1.

A view of the complex is given in Figure 2 and Table 1 reports selected bond distances and angles found in $\text{Co}(\text{hfac})_2 \cdot 2\text{H}_2\text{O} \cdot \text{tetraglyme}$. The cobalt cation is *esa*-coordinated by the four oxygen atoms of two hfac anions

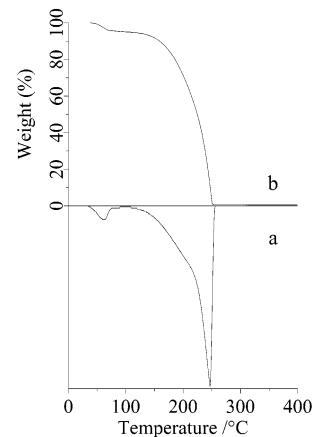


Figure 3. DTG (a) and TG (b) analyses of $\text{Co}(\text{hfac})_2 \cdot 2\text{H}_2\text{O} \cdot \text{tetraglyme}$.

Table 2. Intermolecular Hydrogen Bond Distances (Å) and Angles (deg) for $\text{Co}(\text{hfac})_2 \cdot 2\text{H}_2\text{O} \cdot \text{tetraglyme}$

$\text{Ox} \cdots \text{Hox} \cdots \text{Oy}^a$	Hox \cdots Oy bond distance	Ox \cdots Hox \cdots Oy bond angle
O5–Ho5a \cdots O7	1.88(8)	166(7)
O5–Ho5b \cdots O9	2.08(7)	162(8)
O6–Ho6a \cdots O8'	1.99(8)	169(8)
O6–Ho6b \cdots O11'	1.58(10)	165(8)

^a ' = x, y = 1, z.

and by the oxygens of the two water molecules. The coordination geometry around the cation is a regular octahedron. Co–O bond distances are all comparable and lie in the range 2.065(4)–2.096(5) Å (see Table 1). An analysis carried out using the Cambridge Crystallographic Database v.5.23 (CSD) showed that all the observed Co–O bond distances are in agreement with those found for cobalt complexes having water molecules (range 2.004–2.236 Å, mean value 2.099) or hfac anions (range 2.019–2.108 Å, mean value 2.050) as ligands.³⁰ The hfac anions C–C bond distances (1.392–1.410 Å) evidenced the presence of π resonance.^{17–20} The tetraglyme molecule does not coordinate to the metal, but interacts with the two water molecules. In fact, the O7 and O9 atoms give rise to short intermolecular hydrogen bonds with the Ho5a and Ho5b atoms linked to O5. The atoms O8 and O11, on the other hand, interact with the hydrogen atoms Ho6a' and Ho6b' linked to the oxygen atoms O6' (' = x, y = 1, z) (Table 2). The $\text{Co}(\text{hfac})_2 \cdot 2\text{H}_2\text{O}$ units are bridged together by tetraglyme molecules, and a chain along the y axis takes place (see Figure 2). Finally, the tetraglyme molecule assumes a U conformation as a consequence of the hydrogen bonds involving the oxygen atoms of the polyether.

The thermal behavior of the $\text{Co}(\text{hfac})_2 \cdot 2\text{H}_2\text{O} \cdot \text{tetraglyme}$ was investigated by thermal (TGA) and differential gravimetric analysis (DTG) under 1 atm of prepurified nitrogen, using a 2 °C/min heating rate in the 20–400 °C range (Figure 3). Results show two mass loss processes in the 35–80 and 110–255 °C ranges. The lower temperature process has associated a minor (\approx 5%)

(30) (a) Allen, F. H.; Kennard, O. Cambridge Structural Database. *Chem. Soc. Perkin Trans. 2* **1989**, 1131. (b) Crystallographic data for the structure reported in the present paper have been deposited with the Cambridge Crystallographic Data Centre as supplementary publication no. CCDC-204458. Copies of the data can be obtained on application to CCDC, 12 Union Road, Cambridge CB2 1EZ, UK (Fax: +44-1223-336-033. E-mail: deposit@ccdc.cam.ac.uk).

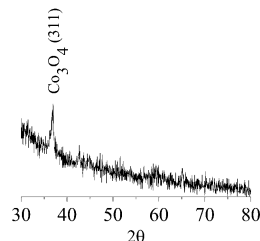
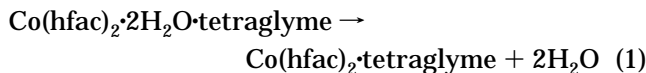


Figure 4. X-ray diffraction pattern, over a $30^\circ < 2\theta < 80^\circ$ angular range, for representative SiO_2 -supported, Co_3O_4 as-deposited thin films.

mass loss which, however, is nicely tuned with the following equation:



A close dehydration temperature has been reported for $\text{Co}(\text{hfac})_2 \cdot 2\text{H}_2\text{O}$.^{17a} The remaining 95% mass is lost quantitatively in the second step, without residue left. Therefore, the lower temperature process leaves an anhydrous, liquid adduct, which evaporates intact afterward.²⁰ Identical conclusions have been arrived at by the gas-phase IR data discussed above.

MOCVD experiments were performed using a horizontal hot-wall reactor,^{17–20} under reduced pressure, using the present, crystallized, $\text{Co}(\text{hfac})_2 \cdot 2\text{H}_2\text{O} \cdot \text{tetraglyme}$ adduct as the liquid Co source. Fused SiO_2 (quartz) was used as the substrate after cleaning in an ultrasonic bath with isopropyl alcohol. Optimized MOCVD conditions require pure Ar (100 sccm) and O_2 (400 sccm) as carrier and reaction gases, respectively. The total pressure, kept in the 2–5 Torr range, was measured using a MKS Baratron 122AAX system. Flow rates were controlled within ± 2 sccm using MKS flow controllers and a MKS 147 multigas controller. Evaporation rates of the source precursor, suited for MOCVD experiments (~ 4 mg/min), were found in the 110 °C range. The substrate temperature was maintained at 400 °C and the deposition time was 120 min.

XRD measurements (Figure 4) of as-deposited films always provide evidence of poor crystalline (311) textured Co_3O_4 phases in the adopted MOCVD condition.³¹ Similar texturing has already been observed in Co_3O_4 films obtained by CVD using other β -diketonate precursors.^{7c,15a,17a} Present XRD measurements further confirm and show enhanced behavior. A qualitative estimation of the mean crystallite sizes, from the XRD line broadening,^{15a,17–20,32–34} gives 8 nm. This value indicates that present films are nanostructured.^{15a} The optical spectrum of as-deposited Co_3O_4 films is reported in Figure 5 and finds counterparts in previously reported data.^{4,5,7c,13b,e,g,14a,15a} The results give evidence that the film absorbance gradually decreases while increasing the wavelength on going from visible to the near-IR range.^{14a} The absorption band at $\lambda = 729$ nm,

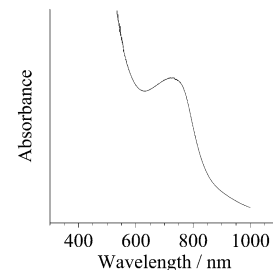


Figure 5. Optical spectrum for a representative Co_3O_4 thin film on a SiO_2 substrate.

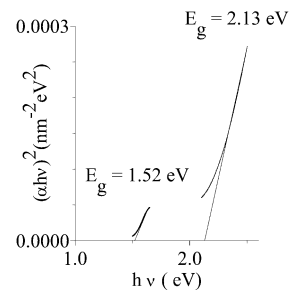


Figure 6. Plot $(\alpha h\nu)^2$ vs $h\nu$ for a representative as-deposited Co_3O_4 film.

in agreement with already reported literature data, is due to a ligand-to-metal charge-transfer $\text{O}(\text{II}) \rightarrow \text{Co}(\text{III})$.^{15a} The film thickness has been evaluated from UV-visible data ($370 \text{ nm} \pm 10\%$ for 120-min experiments) using the classical Swanepoel's algorithms. The resulting growth rate of the Co_3O_4 films is about 30 Å/min.^{15a,17–20,35}

One of the main results, obtained by careful analysis of the absorption coefficient for this material, is the estimation of the so-called optical energy gap by using a classical Tauc approach.^{4,14a,b,15a} Figure 6 shows the Tauc plot $(\alpha h\nu)^2$ vs $h\nu$ for a representative as-deposited Co_3O_4 film. It has been well-established that for a large number of semiconductors the dependence of the absorption coefficient α , for the high-frequency region, upon the photon energy $h\nu$, for optically induced transitions, is given by the following classical expression,^{4,14a,b,15a}

$$\alpha h\nu = k(h\nu - E_g)^n$$

where E_g represents the optical band gap, $h\nu$ is the photon energy, k is a constant, and n depends on the nature of the transition. In fact, n assumes values of $1/2$, $3/2$, 2 , and 3 for allowed direct, forbidden direct, allowed indirect, forbidden indirect transitions, respectively. In the present case, the best fit of $(\alpha h\nu)^{1/n}$ vs the photon energy was obtained for $n = 1/2$. Two straight-line portions have been observed with intercepts at 2.13 and 1.52 eV, thus suggesting that the deposited Co_3O_4 films are semiconducting with allowed direct transitions at these energies. Both obtained values are close to others previously reported for Co_3O_4 films.^{4,14a,b,15a}

Figure 7 shows the Al K α XPS of a representative as-deposited cobalt oxide film in the Co 2p, O 1s binding energy (B.E.) regions.^{2,14h,15a,36} The Co 2p features consist of the main $2p_{1/2}$, $2p_{3/2}$ spin-orbit components at 795.8 and 780.7 eV, respectively.^{2,36} Moreover, weak

(31) American Society for Testing and Material, Powder Diffr. Files, Joint Committee on Powder Diffr. Standards, USA, 1971; #9-402 and #9-418.

(32) Gulino, A.; La Delfa, S.; Fragalà, I.; Egddell, R. G. *Chem. Mater.* **1996**, *8*, 1287.

(33) Gulino, A.; Fragalà, I. *Chem. Mater.* **2002**, *14*, 116.

(34) (a) Jiang, H. G.; Rühle, M.; Lavernia, E. J. *J. Mater. Res.* **1999**, *14*, 549. (b) Warren, B. E. *X-ray Diffraction*; Addison-Wesley: Reading, MA, 1969.

(35) Swanepoel, R. *J. Phys. E: Sci. Instrum.* **1983**, *16*, 1214.

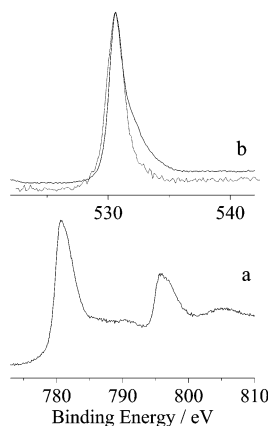


Figure 7. Al K α excited XPS of a representative Co₃O₄ thin film measured in the (a) Co 2p and (b) O 1s energy regions. Solid line of O 1s refers to films before sputtering; dotted line refers to films after 1 min of sputtering. Structures due to satellite radiation have been subtracted from the spectra.

shake-up satellites, centered at 790.5 and 805.6 eV, about 10 eV from the main bands, characteristic of the Co₃O₄ phase, are evident in Figure 7a.^{2,36} The O 1s peak at 530.6 eV shows a shoulder at 531.9 eV (Figure 7b). These features are identical to those already reported for related Co₃O₄ systems and are due to the presence of hydroxide species on the surface, which are ubiquitous in air-exposed cobalt oxide materials.^{2,36}

Depth profiles, obtained by alternating XPS core level measurements with Ar⁺-ion sputter etching (4 kV, beam

current 1.0 μ A) every 60 s, show the absence of any bulk carbon and fluorine contamination. Moreover, after 1 min of sputtering, only the 530.6 eV O 1s component remains evident, due to removal of hydroxide surface species (Figure 7b).

In conclusion, to the best of our knowledge, this study represents the first synthesis of a liquid, at MOCVD conditions, cobalt complex useful for deposition of cobalt oxides. The novel [Co(hfac)₂·2H₂O·tetraglyme] adduct undergoes a dehydration process at low temperature followed by the quantitative evaporation of the anhydrous [Co(hfac)₂·tetraglyme] system. Deposition experiments using this liquid precursor (at MOCVD condition) result in Co₃O₄ (311) oriented thin films. Present cobalt oxide films show both high absorbance in the visible range and low emission in the infrared range, thus representing good candidates for application in the thermal solar energy conversion devices and as anodic electrochromic materials.

Acknowledgment. The authors thanks the Consiglio Nazionale delle Ricerche (CNR Roma) and the Ministero Istruzione Università e Ricerca (MIUR, Roma) for financial support. Prof. S. Giuffrida is gratefully acknowledged for UV-vis measurements. The Centro Interdipartimentale di Cristallografia Strutturale (Cristallografia Strutturale (CRIST), University of Florence, where the X-ray measurements were performed, is gratefully acknowledged.

Supporting Information Available: Table S1, crystal data and structure refinement for Co(hfac)₂·2H₂O·tetraglyme (PDF). X-ray crystallographic file (CIF) of the Co(C₅F₆HO₂)₂·2H₂O·CH₃(OCH₂CH₂)₄OCH₃ structure. This material is available free of charge via the Internet at <http://pubs.acs.org>.

CM034305Z

(36) (a) Kim, K. S. *Phys. Rev. B* **1975**, *11*, 2177. (b) Chuang, T. J.; Brundle, C. R.; Rice, D. W. *Surf. Sci.* **1976**, *59*, 413. (c) McIntyre, N. S.; Cook, M. G. *Anal. Chem.* **1975**, *47*, 2208. (d) Jiménes, V. M.; Fernández, A.; Espinós, J. P.; González-Elipe, A. R. *J. Electron Spectrosc. Relat. Phenom.* **1995**, *71*, 61. (e) Nefedov, V. I.; Firsov, M. N.; Shaplygin, I. S. *J. Electron Spectrosc. Relat. Phenom.* **1982**, *26*, 65.